



Mobility of the {0110} inversion domain boundary in ZnO nanopillars

Jun Wang^{a,*}, Min Zhou^{b,*}, Rong Yang^a, Pan Xiao^a, Fujiu Ke^c, Chunsheng Lu^d

^a State Key Laboratory of Nonlinear Mechanics (LNM), Institute of Mechanics, Chinese Academy of Sciences, Beijing 100190, China

^b G.W.W. School of Mechanical Engineering, Georgia Institute of Technology, Atlanta, GA 30332-0405, United States

^c School of Physics, Beihang University, Beijing 100191, China

^d School of Civil and Mechanical Engineering, Curtin University, Perth, WA 6845, Australia

ARTICLE INFO

Keywords:

ZnO
Inversion domain boundary
Apparent activation energy
Microstructure
Simulation and modelling

ABSTRACT

The apparent activation energy of a nanostructure is difficult to directly measure experimentally. In this letter, we present a computational method for estimating the apparent activation energy of a range of semiconductor nanostructures. This method allows the activation energy to be obtained from experimentally measured average activation time or propagation speed at various temperatures of the phase boundary associated with the transformation. The approach entails analyzing the mobility of the transformation in question using a model based on the Arrhenius relation. The specific analysis carried out uses the {0110} inversion domain boundary in wurtzite ZnO nanopillars as example. Molecular dynamics simulations are conducted over the temperature range of 300–900 K of the corresponding available experimental data. The approach and analysis offer a means for experimentally establishing the apparent activation energy of the {0110} inversion domain boundary in a variety of wurtzite-structured II-VI, III-V and IV-IV binary compounds.

Inversion domain boundaries (IDBs) in wurtzite-structured II-VI, III-V and IV-IV binary compounds, especially in ZnO nanostructures, have attracted a continuing interest for their tailoring roles in the electrical properties such as electron transport [1] and p-type conductivity [2], and thermal properties like phonon scattering [3]. This is because the occurrence of an IDB results in distortion of local lattice structures around it and leads to polarization inversion at its two sides. Tuning properties via distortion of local lattice structures are also adopted in metals [4,5], alloys [6] and ceramics [7]. Therefore, it is necessary to ascertain the thermal stability or mobility of an IDB at finite temperature, as its participation can alter electrical, thermal and mechanical properties of ZnO nanostructures. So far, there are two types of IDBs experimentally observed in ZnO nanostructures. One type happens on the {0001} planes due to doping of other elements such as Sn and Sb [8] and the other type appears in pristine ZnO on the {0110} planes (hereafter referred to as the {0110} IDB) [9] (see Fig. 1 generated by the VMD software [10]). To the best of our knowledge, there are a few works refer to the thermal stability of the former [11], but the mobility of the {0110} IDB in ZnO remains unexplored.

In this Letter, we combined molecular dynamics simulations with available experimental data to investigate the mobility of the {0110} IDB in wurtzite ZnO nanopillars at temperatures ranging from 300 to

900 K. By fitting the Arrhenius equation to the average activation time of the {0110} IDB from molecular dynamics results and experimental data, the analysis was carried out to yield the apparent activation energy of the {0110} IDB and the vibrational frequency of wurtzite ZnO. Then, the average speed of the {0110} IDB was derived. The fitted values of the apparent activation energy and activation frequency were verified by the available energy barrier between the wurtzite and tetragonal phases of ZnO [12] and phonon spectrum of wurtzite ZnO [13] via density functional theory calculations. Finally, potential applications were discussed to experimentally determine the apparent activation energy of the {0110} IDBs in wurtzite-structured II-VI, III-V and IV-IV binary compounds.

As shown in Fig. 2, four activation events of the {0110} IDB in a wurtzite-structured ZnO nanopillar are observed with an average activation time of 165 ns at 600 K (see Supplementary Material S1 for simulation details). It spontaneously hops to and finally annihilates on surface of the nanopillar. As temperature rises to 900 K, the average activation time reduces to 1.2 ns (Fig. 3a). One-time activation of the {0110} IDB can be regarded as the two oppositely structural transformations at two sites simultaneously. One is that from a four-atom ring to two wurtzite Zn-O pairs at the {0110} IDB. The other is the opposite transformation occurring at its neighboring wurtzite cells (see inset in

* Corresponding authors.

E-mail addresses: wangjun@lnm.imech.ac.cn (J. Wang), min.zhou@gatech.edu (M. Zhou).

<https://doi.org/10.1016/j.matlet.2021.130778>

Received 3 July 2021; Received in revised form 20 August 2021; Accepted 25 August 2021

Available online 30 August 2021

0167-577X/© 2021 Elsevier B.V. All rights reserved.

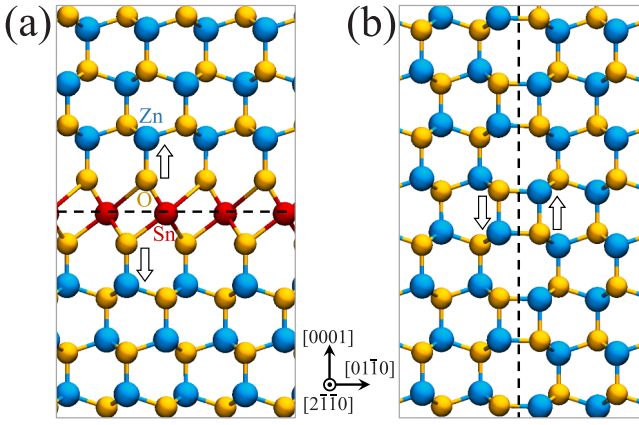


Fig. 1. (a) The {0001} and (b) {0110} IDBs (indicated by dash lines) in wurtzite-structured ZnO. Hollow arrows show the polarity of axial Zn-O pairs along the [0001] orientation.

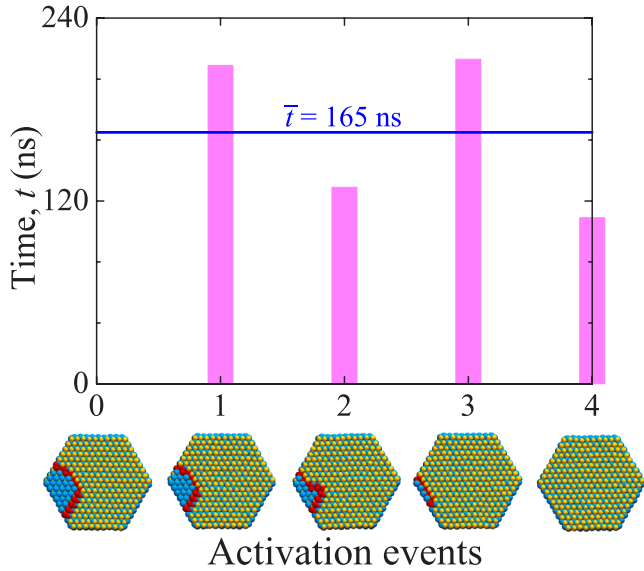


Fig. 2. The {0110} IDB (outlined in red) hops four times with an average activation time of 165 ns to annihilate on surface of the nanopillar, which is annealed at a temperature of 600 K.

Fig. 3b). Since the {0110} IDB and the tetragonal structure [12] of ZnO possess the same building unit (the four-atom ring), the average activation time of the {0110} IDB at 300 K can be supposed to the time scale (~ 10 s) of the reversible tetragonal-to-wurtzite phase transformation experimentally measured in ZnO nano-islands at room temperature [12].

Given that the apparent activation energy of the {0110} IDB is ΔE , the activation frequency γ at temperature T can be described by the Arrhenius equation

$$\gamma = \gamma_0 e^{-\frac{\Delta E}{k_B T}}, \quad (1)$$

where γ_0 and k_B are the vibrational frequency of a crystal and the Boltzmann constant, respectively. Therefore, the average activation time \bar{t} at which one can observe an activation event is $\bar{t} = 1/\gamma$, that is

$$\bar{t} = \frac{1}{\gamma_0} e^{\frac{\Delta E}{k_B T}} \quad (2)$$

In practice, \bar{t} and ΔE are regarded as the input and output variables, respectively. The values of $\Delta E = 0.87$ eV and $\gamma_0 = 3.5 \times 10^{13} \text{ s}^{-1}$ are obtained by fitting the values of \bar{t} from molecular dynamics simulations

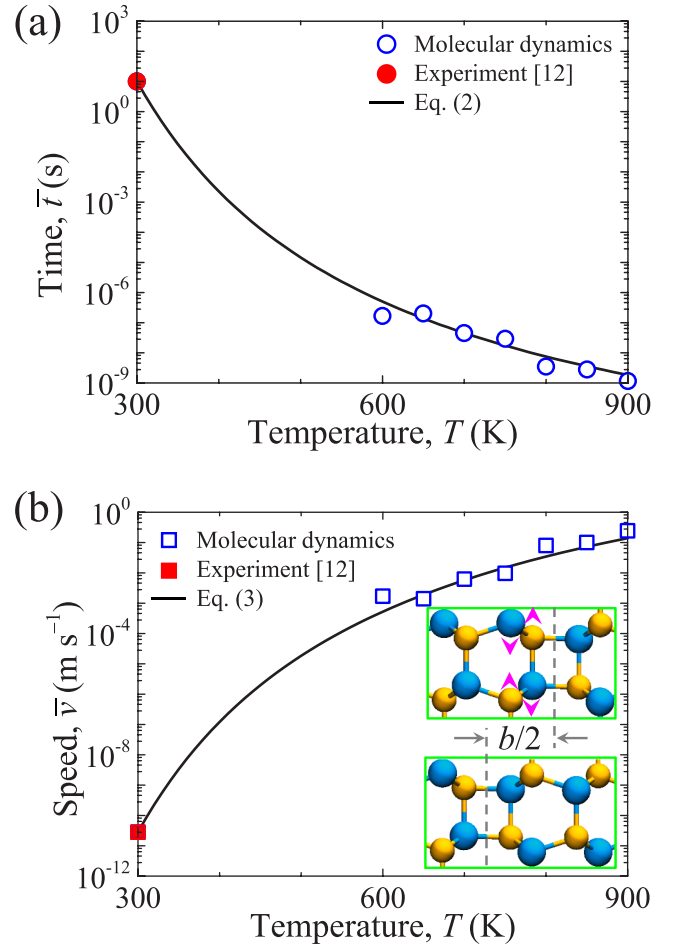


Fig. 3. (a) The average activation time of the {0110} IDB and (b) its propagation speed vary with temperature. Inset shows that at each activation the {0110} IDB (denoted by dash lines) moves by $b/2$, with b the lattice constant of wurtzite ZnO. Arrow heads show the directions of atomic motions during the activation.

at $600 \text{ K} \leq T \leq 900 \text{ K}$ and the experimental data at $T = 300 \text{ K}$ [12]. The fitted value of γ_0 is consistent with the upper limit frequency scale of optical phonons in wurtzite ZnO [13]. Actually, most crystals have a value of γ_0 in the order of 10^{13} s^{-1} .

The value of ΔE can also be solely obtained by computation. Based on the interatomic force field of ZnO [14], it is calculated to be 0.76 eV by molecular statics (see Supplementary Material S2). Moreover, density functional theory calculations have put the energy barrier between wurtzite and tetragonal phases of ZnO at 0.96 eV [12]. It is seen that molecular statics and the density functional theory draw the lower and upper boundaries of ΔE , with the fitted value of 0.87 eV between them.

After each activation, the {0110} IDB travels along the $\langle 0110 \rangle$ orientation by $d = b/2$, with $b = 5.61 \text{ \AA}$ [14] the lattice constant of wurtzite ZnO (see inset in Fig. 3b and Supplementary Video 1). Thus, its average propagation speed is $\bar{v} = d/\bar{t} = b/(2\bar{t})$, or

$$\bar{v} = d\gamma_0 e^{-\frac{\Delta E}{k_B T}}, \quad (3)$$

which grows from 2.8×10^{-11} to $1.4 \times 10^{-1} \text{ m s}^{-1}$ as temperature increases from 300 to 900 K, tracking both simulation results and experimental data in the ten orders of magnitude, as shown in Fig. 3b. It is indicated that, to derive ΔE , \bar{v} can also be regarded as the input variable.

It is worth noting that IDBs are frequently observed in wurtzite II-VI [9], III-V [15] and IV-IV [16] binary compound nanostructures. However, in contrast to computational estimation, there are few experiments

on apparent activation energies. Therefore, it is necessary to develop a practicably experimental protocol to obtain accurate apparent activation energies for engineering applications, which can be solved by Eqs. (2) or (3). Specifically, since \bar{t} , d and \bar{v} are experimentally measurable at various T , ΔE can be determined by the linear relationship of $\ln(\bar{t}) \sim 1/(k_B T)$ or $\ln(\bar{v}) \sim 1/(k_B T)$. Here, an aberration-corrected transmission electron microscopy could be applied to collect \bar{t} , d and \bar{v} around room temperature [12]. However, it is still a challenge on how to introduce a wide and varying range of T (e.g., 300–900 K) in the observation chamber of an aberration-corrected transmission electron microscope.

In summary, the mobility of the {0110} IDB in wurtzite-structured ZnO nanopillars has been modeled by the Arrhenius equation with an average activation time as the input variable and the apparent activation energy as the output. The model can be also adapted to an average speed of the {0110} IDB as the input. The derived apparent activation energy of 0.87 eV of the {0110} IDB in ZnO matches the average activation time of molecular dynamics simulations and available experimental data from 1.2 ns to 10 s in the ten orders of magnitude with temperatures ranging from 300 to 900 K. It is shown that the value of 0.87 eV falls between the computational results of molecular statics and the density functional theory. This work, therefore, provides a guidance for accurately determining the apparent activation energy of the {0110} IDBs in wurtzite-structured ZnO.

CRedit authorship contribution statement

Jun Wang: Conceptualization, Investigation, Methodology, Data curation, Writing - original draft, Writing - review & editing, Funding acquisition. **Min Zhou:** Supervision, Writing - review & editing. **Rong Yang:** Formal analysis, Writing - review & editing. **Pan Xiao:** Funding acquisition, Writing - review & editing. **Fujiu Ke:** Methodology. **Chunsheng Lu:** Formal analysis, Validation, Writing - review & editing.

Declaration of Competing Interest

The authors declare that they have no known competing financial interests or personal relationships that could have appeared to influence the work reported in this paper.

Acknowledgements

This work was supported by the National Natural Science Foundation of China (Grant Nos. 11772332 and 11790292), the Strategic Priority Research Program of the Chinese Academy of Sciences (Project No. XDB22040501) and the Opening Fund of State Key Laboratory of Nonlinear Mechanics. Computations were performed on the resources provided by the Pawsey Supercomputing Center with funding from the Australian Government and the Government of Western Australia, the LNMGrid of the State Key Laboratory of Nonlinear Mechanics and the ScGrid of Supercomputing Center, Computer Network Information Center of the Chinese Academy of Sciences.

Appendix A. Supplementary data

Supplementary data to this article can be found online at <https://doi.org/10.1016/j.matlet.2021.130778>.

References

- [1] J. Hoemke, E. Tochigi, T. Tohei, H. Yoshida, N. Shibata, Y. Ikuhara, Y. Sakka, *J. Am. Ceram. Soc.* 100 (2017) 4252–4262.
- [2] K.C. Pradel, J. Uzuhashi, T. Takei, T. Ohkubo, K. Hono, N. Fukata, *Nanotechnology* 29 (33) (2018), 335204.
- [3] K. Park, J.K. Seong, S. Nahm, *J. Alloy. Comp.* 455 (1–2) (2008) 331–335.
- [4] F. Shuang, K.E. Aifantis, *Acta Mater.* 195 (2020), 358370.
- [5] F. Shuang, K.E. Aifantis, *Appl. Surf. Sci.* 535 (2021), 147602.
- [6] X.W. Li, T. Shi, B. Li, X.C. Chen, C.W. Zhang, Z.G. Guo, Q.X. Zhang, *Mater. Des.* 183 (2019), 108152.
- [7] X.W. Li, J.S. Liang, T. Shi, D.N. Yang, X.C. Chen, C.W. Zhang, Z.H. Liu, D.Z. Liu, Q. X. Zhang, *Ceram. Int.* 46 (9) (2020) 1291112920.
- [8] V. Ribić, A. Rečnik, M. Komelj, A. Kokalj, Z. Branković, M. Zlatović, G. Branković, *Acta Mater.* 199 (2020), 633648.
- [9] Y.Z. Liu, H.T. Yuan, Z.Q. Zeng, X.L. Du, X.D. Han, Q.K. Xue, Z. Zhang, *Philos. Mag. Lett.* 87 (9) (2007), 687693.
- [10] W. Humphrey, A. Dalke, K. Schulten, *J. Mol. Graph.* 14 (1) (1996) 33–38.
- [11] J. Rohrer, K. Albe, *Phys. Rev. Mater.* 5 (2021), 023601.
- [12] M.R. He, R. Yu, J. Zhu, *Angew. Chem.-Int. Edit.* 51 (31) (2012) 7744–7747.
- [13] Z. Wang, F. Wang, L. Wang, Y. Jia, Q. Sun, *J. Appl. Phys.* 114 (6) (2013), 063508.
- [14] S.W. Wang, Z.C. Fan, R.S. Koster, C.M. Fang, M.A. van Huis, A.O. Yalcin, F. D. Tichelaar, H.W. Zandbergen, T.J.H. Vlugt, *J. Phys. Chem. C* 118 (20) (2014) 11050–11061.
- [15] S. Mahanty, M. Hao, T. Sugahara, R.S.Q. Fareed, Y. Morishima, Y. Naoi, T. Wang, S. Sakai, *Mater. Lett.* 41 (2) (1999) 6771.
- [16] M. Zimbone, E.G. Barbagiovanni, C. Bongiorno, C. Calabretta, L. Calcagno, G. Fiscaro, A. La Magna, F. La Via, *Cryst. Growth Des.* 20 (5) (2020) 3104–3111.